

AD-A266 999



OFFICE OF NAVAL RESEARCH  
Contract N/N00014-91-J-1893  
R&T Code 4132062

TECHNICAL REPORT NO. 3

NMR and Theoretical Investigation of Cation Binding  
With Sol-Gel Silicates

by

J. Sanchez and A.V. McCormick  
Dept. of Chemical Engineering & Materials Science  
University of Minnesota  
421 Washington Ave. SE  
Minneapolis, MN 55455

**S** DTIC  
ELECTE  
JUL 19 1993  
**A** **D**

July 12, 1993

Reproduction in whole or in part is permitted for any purpose of the  
U.S. government.

This document has been approved for public release and sale; its  
distribution is unlimited.

8 7 16 146

93-16240  


**REPORT DOCUMENTATION PAGE**

1. AGENCY USE ONLY (Leave blank)		2. REPORT DATE 7/12/93	3. REPORT TYPE AND DATES COVERED Technical	
4. TITLE AND SUBTITLE NMR and Theoretical Investigation of Cation Binding with Sol-Gel Silicates			5. FUNDING NUMBERS N/N00014-91-J-1893	
6. AUTHOR(S) J. Sanchez and A. McCormick				
7. PERFORMING ORGANIZATION NAME(S) AND ADDRESS(ES) Dept. of Chemical Engineering & Materials Science University of Minnesota 421 Washington Ave., SE Minneapolis, MN 55455			8. PERFORMING ORGANIZATION REPORT NUMBER	
9. SPONSORING / MONITORING AGENCY NAME(S) AND ADDRESS(ES) Office of Naval Research 800 N. Quincy Street Arlington, VA 22217			10. SPONSORING / MONITORING AGENCY REPORT NUMBER	
11. SUPPLEMENTARY NOTES Published in Chemistry of Materials, 1991, 3				
12a. DISTRIBUTION / AVAILABILITY STATEMENT Reproduction in whole or in part is permitted for any purpose of the U.S. Government. This document has been approved for public release and sale; its distribution is unlimited.			12b. DISTRIBUTION CODE	
13. ABSTRACT (Maximum 200 words) Previous reports suggest that the choice of base catalyst affects both the kinetics and structural evolution of SiO <sub>2</sub> gelation from tetraethoxysilane (TEOS). Furthermore, these effects have been attributed to the interaction of the alkaline cations with charged silicate fragments. In this study, NMR analysis of alkali-metal nuclei and of <sup>29</sup> Si directly shows that during the condensation of silicon alkoxides in basic alcohol solutions, cations form ion-pair complexes with negatively charged silicate groups. It is determined that the ion pair is formed most favorably with potassium. In seeking a predictive model of complex stability, we found it most successful to use a bond orbital electronegativity equalization model developed by Bergman and Hinze.				
14. SUBJECT TERMS SiO <sub>2</sub> , sol/gel, NMR, electronegativity equalization, cation			15. NUMBER OF PAGES 5	
			16. PRICE CODE	
17. SECURITY CLASSIFICATION OF REPORT unclassified	18. SECURITY CLASSIFICATION OF THIS PAGE unclassified	19. SECURITY CLASSIFICATION OF ABSTRACT unclassified	20. LIMITATION OF ABSTRACT UL	

# NMR and Theoretical Investigation of Cation Binding with Sol-Gel Silicates

Jorge Sanchez and Alon McCormick\*

Department of Chemical Engineering and Materials Science, University of Minnesota,  
Minneapolis, Minnesota 55455

Received September 11, 1990. Revised Manuscript Received January 2, 1991

Previous reports suggest that the choice of base catalyst affects both the kinetics and structural evolution of SiO<sub>2</sub> gelation from tetraethoxysilane (TEOS). Furthermore, these effects have been attributed to the interaction of the alkaline cations with charged silicate fragments. In this study, NMR analysis of alkali-metal nuclei and of <sup>29</sup>Si directly shows that during the condensation of silicon alkoxides in basic alcohol solutions, cations form ion-pair complexes with negatively charged silicate groups. It is determined that the ion pair is formed most favorably with potassium. In seeking a predictive model of complex stability, we found it most successful to use a bond orbital electronegativity equalization model developed by Bergman and Hinze.

## Introduction

Much of the promise of sol-gel technology rests on the development of reaction engineering models. Therefore, we are interested in a detailed understanding of the kinetics and mechanism of sol-gel reactions. One particularly important aspect is how the catalyst affects both the overall kinetics and the structural evolution of reacting silicon alkoxides. For instance, the use of NaOH as a catalyst instead of NH<sub>4</sub>OH results in a slower condensation and a more complete conversion of tetramethoxysilane.<sup>2</sup> The gel microstructure and properties can also depend strongly on the type of base used. For example, though base-catalyzed silicon alkoxide gels are generally not spinnable,<sup>3</sup> we have observed that when KOH is the catalyst, spinnable gels are formed, whereas this is not the case when the catalyst is NaOH or NH<sub>4</sub>OH.

McCormick et al.<sup>4</sup> have previously used NMR spectroscopy to show that alkali-metal cations participate in the condensation of silicate anions in aqueous solution. Such a mechanism may also be operative for sol-gel condensation in solution containing both alcohol and water. In basic conditions, the hydrolyzed alkoxide deprotonates to form anionic groups much like those found in aqueous silicate solutions. We have previously found that the concept of ion pairing helps to account for apparent activation energies of silicon alkoxide gelation reactions under conditions where the gelation results from cluster-cluster condensation.<sup>5-7</sup>

In this study, we present cation NMR evidence of ion-pair complexation in base-catalyzed sol-gel systems, comprised of TEOS, water, and ethanol. The cation NMR lines allow us to deduce whether the cation is coordinated to ethanol, water, or silicates. Furthermore, we test three theoretical models to predict the stability of the ion pair that is detected by NMR spectroscopy. First, we consider a simple electrostatic model based on formal charges.

Second, we use a model developed by Livage and Henry.<sup>8</sup> These authors have pioneered the application of electronegativity equalization to predict sol-gel precursor reactivities through the use of a partial charge model based on Allred-Rochow electronegativities and Sanderson's principle of electronegativity equalization. However, this model might not successfully predict the current results. Finally, we consider a model proposed by Bergmann and Hinze,<sup>1</sup> which is based on bond orbital electronegativity equalization (BOEE). We show that this model predicts complex stability in accord with experiment.

## Theory

**NMR Spectra of Alkali-Metal Nuclei.** NMR spectroscopy is a powerful quantitative tool to study the chemistry of the group Ia elements.<sup>9,38</sup> In spite of high nuclear quadrupole moments, solvated alkali-metal cations ordinarily give sharp single NMR signals. This is attributed to the high symmetry and mobility of solvated cations.<sup>9,38</sup> However, alkali-metal ions are known for their ability to form ionic complexes. The nuclei of cations complexed with ionophores (e.g., valinomycin, crown ethers, cryptands) or strongly binding anions can relax quickly as the cation loses its symmetrical environment and mobility.<sup>10-12</sup> This broadens the NMR signal, sometimes even beyond detection. For example, Shporer et al.<sup>13</sup> were unable to detect the signal of <sup>23</sup>Na complexed with valinomycin. In this case, the "disappearance" of the NMR signal indicates that the cation has complexed. Alkali-metal NMR spectroscopy has also been used successfully to observe cation complexation with a number of organic acids<sup>14,15</sup> and silicate oligomers in basic aqueous solution.<sup>4</sup>

**Partial Charge Distribution Calculation.** Livage et al.<sup>8,16</sup> have employed partial charge distribution calcula-

(1) Bergmann, D.; Hinze, J. *Struct. Bonding* 1987, 66, 145-190.  
(2) Kelts, L. W.; Effinger, N. J.; Melpolder, S. M. *J. Non-Cryst. Solids* 1984, 63, 353.  
(3) Brinker, C. J. *J. Non-Cryst. Solids* 1988, 100, 31.  
(4) McCormick, A. V.; Bell, A. T.; Radke, C. J. In *Better Ceramics through Chemistry III*; Brinker, C. J., Ed.; Material Research Society Spring Meeting, Reno, April 1988.  
(5) Schaefer, D. W. *MRS Bull.* 1988, 8, 22.  
(6) Assink, R. A. In *Better Ceramics through Chemistry*; Brinker, C. J., Ed.; Wiley: New York, 1984; p 301.  
(7) Sanchez, J.; Reese, M. E.; McCormick, A. V. In *Better Ceramics through Chemistry IV*; Brinker, C. J., Ed.; Material Research Society Spring Meeting, San Francisco, April 1990.

(8) Livage, J.; Henry, M. In *Ultrastructure Processing of Advanced Ceramics*; Ulrich, D. R., Ed.; Wiley: New York, 1988; p 183.  
(9) Lindmann, B.; Forsén, S. In *NMR and the Periodic Table*; Harris, R. K., Ed.; Academic Press: New York, 1978.  
(10) Grotans, A. M.; Smid, J.; DeBoer, E. *Chem. Commun.* 1971, 759.  
(11) Haynes, D. H.; Pressman, B. C.; Kowalsky, A. *Biochemistry* 1971, 10, 852.  
(12) Dye, J. L.; Andrews, C. W.; Ceraso, J. M. *J. Phys. Chem.* 1978, 79, 3076.  
(13) Shporer, M.; Poupko, R.; Luz, Z. *Inorg. Chem.* 1972, 11, 2441.  
(14) James, T. L.; Noggle, J. H. *J. Am. Chem. Soc.* 1969, 91, 3424.  
(15) Rechnitz, G. A.; Zamochnick, S. B. *J. Am. Chem. Soc.* 1964, 86, 2953.  
(16) Sanchez, C.; Livage, J.; Henry, M.; Babonneau, F. *J. Non-Cryst. Solids* 1988, 100, 65.

Table I. Electronegativity Parameters Used<sup>a</sup>

group	$b_0$	$b_1$	$c$
Li	7.778		2.386
Na	7.436		2.297
K <sup>+</sup>	6.261		1.920
Rb	6.022		1.846
C <sup>+</sup>	5.99		1.712
O	6.412	15.201	9.371
H <sub>2</sub> O	51.183	17.630	10.825
Si	16.373	7.466	4.557
Li <sup>+</sup>	110.73		35.115
Na <sup>+</sup>	64.366		21.076
K <sup>+</sup>	45.545		13.735
Rb <sup>+</sup>	39.161		11.662
C <sup>+</sup>	35.703		10.603

<sup>a</sup>All values after Bergmann et al.<sup>1</sup> except  $b$  calculated from Moore's ionization potentials<sup>26</sup> and Hotop's electron affinities.<sup>27</sup> The values for O were adjusted for a 140° Si-O-Si bond angle (41% s character). The values for H<sub>2</sub>O are for the lone pair of electrons of the oxygen atom.

tions to predict the reactivity of various sol-gel intermediates. Their method is based on the Allred-Rochow atomic electronegativity scale<sup>17</sup> and on Sanderson's principle of electronegativity equalization.<sup>18</sup> Although very successful in some cases, this model does not account for changes in charge distributions in response to changes in molecular structure and bonding. Moreover, Allred-Rochow electronegativities do not include such important parameters as the electronic valence state and orbital polarizability.<sup>19</sup> More elaborate methods to calculate charge distributions have been proposed; they allow a variation of the electronegativity with orbital hybridization.<sup>20,21</sup> In some models, a partial equalization of electronegativity is used.<sup>22-24</sup> Bergmann and Hinze<sup>1</sup> have proposed a model to obtain charge distributions based on the orbital electronegativities calculated by Hinze and Jaffé.<sup>19,25</sup> They considered a linear relationship between the electronegativity of an orbital  $i$  and its charge  $q_i$  ( $q_i = 0, -1$  or  $-2$  for an empty, singly, or doubly occupied orbital, respectively):

$$\chi_i = b + 2cq_i \quad (1)$$

where  $b = (3I - A)/2$ ,  $c = (I - A)/2$ , and  $I$  and  $A$  are the ionization potential and electron affinity of the considered orbital. For each two-electron bond A-B formed by the orbital  $i$  of the atom A and the orbital  $j$  of the atom B, the equalization of electronegativity is given by

$$\chi_i(q_i + \Delta q_i) = \chi_j(q_j + \Delta q_j) \quad (2)$$

where  $\Delta q_i$  and  $\Delta q_j$  are the charge shifts on the orbitals  $i$  and  $j$ .

To conserve charge

$$\Delta q_i = -\Delta q_j \quad (3)$$

For  $n$  bonds, a system of  $n$  linear equations is obtained and solved numerically for the  $\Delta q_i$ 's. The total net charge on the originally neutral atom A will be

$$Q(A) = \sum_i \Delta q_i \quad (4)$$

(17) Allred, A. L.; Rochow, E. G. *J. Inorg. Nucl. Chem.* 1958, 5, 264.

(18) Sanderson, R. T. *Science* 1961, 114, 670.

(19) Hinze, J.; Jaffé, H. H. *J. Am. Chem. Soc.* 1962, 84, 540.

(20) Hulse, J. J. *Phys. Chem.* 1968, 69, 3294.

(21) Bratsch, S. G. *J. Chem. Educ.* 1985, 62, 101.

(22) Gasteiger, J.; Marilli, M. *Tetrahedron* 1980, 36, 3219.

(23) Mortier, W. M. *Struct. Bonding* 1987, 66, 125.

(24) Mullay, J. *Struct. Bonding* 1987, 66, 1.

(25) Hinze, J.; Jaffé, H. H.; Whitehead, M. A. *J. Am. Chem. Soc.* 1963, 85, 148.

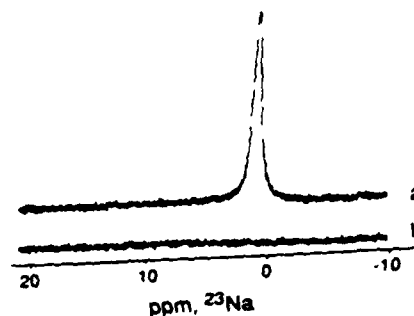


Figure 1. <sup>23</sup>Na NMR spectra for the systems (in molar ratios) 5EtOH/1H<sub>2</sub>O/0.1NaOH (top spectrum) and 1TEOS/4EtOH/1H<sub>2</sub>O/0.1NaOH after 5 min of reaction (bottom spectrum).

The model can be improved by considering a linear dependence between the parameter  $b$  and the "rest charge"  $r_i$ :

$$b = b_0 + b_1 r_i \quad (5)$$

where

$$r_i(A) = Q(A) - \Delta q_i \quad (6)$$

Table I gives the values of  $b_0$ ,  $b_1$ , and  $c$  used in our calculations.

This method accounts very well for the inductive and polarizing effects of chemical groups. It also distinguishes between different molecular structures or isomers.

**Correlation of Partial Charges with Bond Energy and Bond Length.** In the case of reactions involving polar interactions, partial charges allow prediction of the reactivity of atoms or sites in relation with their nucleophile or electrophile character. Partial charge calculations can also be used to estimate the Coulombic contribution to a bond energy, which is given by

$$E_C = \frac{Q^+ Q^-}{4\pi\epsilon_0 r} \quad (7)$$

where  $Q^+$  and  $Q^-$  are the partial charges on respectively the positively and negatively polarized atom in the bond,  $\epsilon_0$  is the vacuum permittivity, and  $r$  is the bond length. According to Derflinger and Polanski,<sup>28</sup> the bond length is approximately determined by the shortening of the purely covalent bond length by the charge shift. Shomaker and Stephenson<sup>29</sup> have shown that the bond length  $d_{AB}$  can be estimated with the relation

$$d_{AB} = r_A + r_B - k|\chi_A - \chi_B| \quad (8)$$

where  $r_A$  and  $r_B$  are the covalent radii of the atoms,  $\chi_A$  and  $\chi_B$  are their electronegativities, and  $k$  is a proportionality constant between the bond shortening by electron transfer and the electronegativity difference of the atoms. Bergmann and Hinze<sup>1</sup> determined that  $k$  does not depend on the bond type and it is a constant equal to 1.9 pm/V (when the electronegativities are in volts). The above formula has successfully predicted bond lengths for more than 120 compounds within a standard deviation of 4 pm. The covalent radii given by Sanderson<sup>30</sup> have been used in the eq 8 for our calculations.

(26) Moore, C. E. *Atomic Energy Levels. Natl. Bur. Stand. (U.S.) Circ.* 1947, No. 467.

(27) Hotop, H.; Lineberger, W. C. *J. Phys. Chem. Ref. Data* 1975, 4, 539.

(28) Derflinger, G.; Polanski, O. E. *Theor. Chim. Acta (Berlin)* 1963, 1, 308.

(29) Shomaker, V.; Stephenson, D. P. *J. Am. Chem. Soc.* 1961, 63, 37.

(30) Sanderson, R. T. *Chemical Bonds and Bond Energy*, 2nd, ed.; Academic Press: New York, 1976.

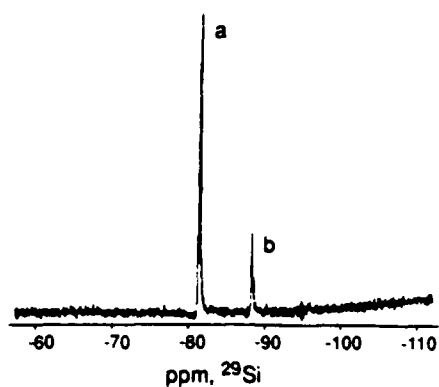


Figure 2.  $^{29}\text{Si}$  NMR spectrum for the system (in molar ratios) 1TEOS/4EtOH/1H<sub>2</sub>O/0.1NaOH after 4 h of reaction: (a) TEOS signal; (b) (EtO)<sub>3</sub>-Si-O-Si-(OEt)<sub>3</sub>.

### Experimental Section

Tetraethoxysilane (TEOS), ethanol, water, and a base catalyst, either NaOH or RbOH, were mixed with various molar ratios in polypropylene vessels at 20 °C. After the sample was transferred to a 10-mm glass NMR tube,  $^{23}\text{Na}$  NMR spectra were acquired at 132.283 MHz with 100 pulses of 31.5  $\mu\text{s}$  and a delay of 1 s between pulses. Chemical shifts were referred to NaOH 50 wt % in water.

$^{87}\text{Rb}$  NMR spectra were acquired at 163.634 MHz, with 1000 pulses of 28  $\mu\text{s}$  and a delay of 0.1 s between pulses. Chemical shifts were referred to RbOH 50 wt % in water.

$^{29}\text{Si}$  NMR spectra were recorded at 99.348 MHz with 100 scans of 25  $\mu\text{s}$  and a pulse delay of 3 s. Peaks were referred to tetramethylsilane (TMS). Cr(acac)<sub>3</sub> was used as a paramagnetic relaxing agent to reduce the spin-lattice relaxation time of  $^{29}\text{Si}$  and, thus, to ensure quantitative spectra.

### Results and Discussion

**NMR Evidence of Ion Pairing.** Figure 1 shows  $^{23}\text{Na}$  spectra at various points in the sample preparation. Before TEOS addition, the  $^{23}\text{Na}$  line is narrow, indicating that the cations are fully solvated and are moving freely in the solution (top spectrum). The line width indicates that it is solvated by water rather than ethanol.<sup>30</sup> Immediately upon addition of TEOS, the sodium signal both diminishes and broadens drastically, either because of the introduction of asymmetry in the cation environment or because of a lowered mobility resulting from complexation. As the reaction proceeds, the cation resonance virtually disappears (bottom spectrum). The corresponding  $^{29}\text{Si}$  NMR spectrum (Figure 2) shows no hydrolyzed TEOS. Thus, as TEOS is hydrolyzed, it quickly polymerizes to dense particles such as those detected by X-ray scattering<sup>5</sup> and electron microscopy.<sup>31</sup>  $^{29}\text{Si}$  signals from these particles do not readily appear in these high-resolution spectra because (i) the fully condensed (Q<sub>4</sub>) and surface (Q<sub>3</sub>) Si sites are broad due to chemical shift distributions, (ii) they would relax slowly because of limited Cr<sup>3+</sup> access,<sup>32</sup> and (iii) they are partly hidden by the broad signal from the glass NMR tube. We deduce that the sodium cations become complexed with negatively charged groups (deprotonated Q<sub>3</sub> silanols) on the colloidal particles. The absence of any narrow  $^{23}\text{Na}$  signal proves that no Na<sup>+</sup> cations are free in solution, although substantial amounts of TEOS remain (even well after gelation).

RbOH catalyzed systems exhibit the same kind of behavior (Figure 3). Incidentally, we note that as the condensation reaction nears completion, Si-O<sup>-</sup>-Rb<sup>+</sup> bonds are

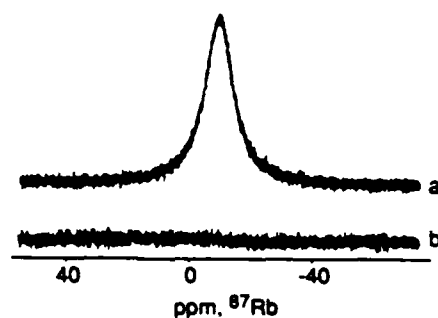


Figure 3.  $^{87}\text{Rb}$  NMR spectra for the systems (in molar ratios) 5EtOH/1H<sub>2</sub>O/0.1RbOH (top spectrum) and 1TEOS/4EtOH/1H<sub>2</sub>O/0.1RbOH after 5 min of reaction (bottom spectrum).

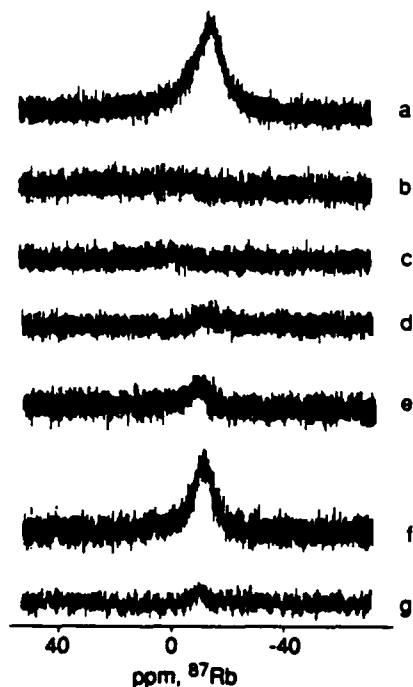


Figure 4.  $^{87}\text{Rb}$  NMR spectra for the systems (in molar ratios): (a) 5EtOH/1H<sub>2</sub>O/0.01RbOH; (b) 1TEOS/4EtOH/1H<sub>2</sub>O/0.01RbOH after 5 min of reaction; (c) same as 4b but with LiCl at saturation; (d) same as 4b but with NaCl at saturation; (e) same as 4b but with NH<sub>4</sub>Cl at saturation; (f) same as 4b but with KCl at saturation; (g) same as 4b but with CsCl at saturation.

replaced by Si-O-Si bonds. Evidently the Si-O-Si bond formation is more favored, but neither water nor ethanol can compete to form Si-OH or Si-OEt bonds.

Summarizing, base cations quickly form stable Si-O<sup>-</sup>...M<sup>+</sup> bonds, even at low cation concentration. These bonds are favored relative to Si-OH and Si-OEt, but they are unfavored relative to Si-O-Si bonds.

**Relative Equilibrium of the Cation Binding.** The relative equilibrium of various ion pairs was investigated by adding alkali-metal chloride salts to RbOH-catalyzed systems. The corresponding  $^{87}\text{Rb}$  NMR spectra are shown in Figure 4. Parts a and b of Figure 4 are the spectra of the system with and without TEOS; as previously shown, the Rb peak disappears when TEOS is added. If LiCl is added, no change occurs (Figure 4c). If NaCl is added, a small amount of Rb<sup>+</sup> is released into solution (Figure 4d). With NH<sub>4</sub>Cl a larger amount is released (Figure 4e). If KCl is added, most of Rb<sup>+</sup> is released (Figure 4f). Finally if CsCl is added, only a small amount of Rb<sup>+</sup> seems to be displaced (Figure 4g). We deduce from Figure 4f that most of the Si-O<sup>-</sup>-Rb<sup>+</sup> bonds have been replaced by Si-O<sup>-</sup>-K<sup>+</sup> bonds.

(31) Bailey, R. K.; Nagase, T.; Broberg, S. M.; Mecartney, M. L. University of Minnesota, personal communication, 1990.

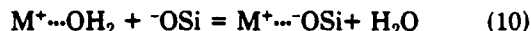
(32) Engelhardt, G.; Radeglia, R. *Chem. Phys. Lett.* 1984, 108, 271.

These spectra suggest the following order of efficacy of the cation at competing for charged surface silicate sites:



**Rationalizing Ion Pair Stabilities.**  $\text{K}^+$  has been observed to produce the fastest condensation of monomeric silicic acid<sup>37</sup> and produces the fastest base-catalyzed TEOS gelations, yielding a spinnable gel. We propose that cation complexation may cause these results. To explain the relative equilibrium of cation-silicate pairs, we next pursue a theoretical investigation.

The ion-pair reaction can be written



where  $\text{M}^+$  is  $\text{Li}^+$ ,  $\text{Na}^+$ ,  $\text{K}^+$ ,  $\text{Rb}^+$ , or  $\text{Cs}^+$ . The reaction represents the competition between a surface silicate group and a water of hydration for the position next to the cation. Note that we are ignoring other waters of hydration, assuming that they will not affect the reaction enthalpy change (for the entropic effect, see below). The physical implications of this simplistic model are considered shortly. We are also assuming that no water of hydration comes between the cation and the silicate fragment. This has been suggested by McCormick et al.<sup>4</sup> The equilibrium constant for ion pairing (ip) is

$$K_{\text{ip}} = e^{-\Delta G_{\text{ip}}/RT} \quad (11)$$

The free energy of reaction is given by

$$\Delta G_{\text{r}} = \Delta H_{\text{r}} - T\Delta S_{\text{r}} = \Delta H_{\text{r}}(\text{M}^+ \cdots \text{OSi}^-) + \Delta H_{\text{r}}(\text{H}_2\text{O}) - \Delta H_{\text{r}}(\text{M}^+ \cdots \text{H}_2\text{O}) - \Delta H_{\text{r}}(\text{OSi}^-) - T\Delta S_{\text{r}} \quad (12)$$

We assume that the entropy change of this reaction is similar for different alkali-metal cations since the reaction entropy will be dominated by changes in the arrangement in water molecules of hydration. The nature of this change is the replacement of hydrating water by the silicate fragment, and we assume that the remaining hydrating water molecules are not affected by the ion-pair complexation. Therefore, only  $\Delta H_{\text{r}}(\text{M}^+ \cdots \text{OSi}^-)$  and  $\Delta H_{\text{r}}(\text{M}^+ \cdots \text{OH}_2)$  change in response to a change of the cation. These two terms are directly related to  $E(\text{M}^+ \cdots \text{OH}_2)$  and  $E(\text{M}^+ \cdots \text{OSi}^-)$ , the energies of the bonds  $\text{M}^+ \cdots \text{OH}_2$  and  $\text{M}^+ \cdots \text{OSi}^-$ . Therefore

$$\Delta H_{\text{r}}(\text{M}^+ \cdots \text{OSi}^-) - \Delta H_{\text{r}}(\text{M}^+ \cdots \text{H}_2\text{O}) \approx E(\text{M}^+ \cdots \text{OH}_2) - E(\text{M}^+ \cdots \text{OSi}^-) \equiv \Delta E \quad (13)$$

Thus  $\Delta E$  is proportional to  $-\ln K_{\text{ip}}$ ; the more negative  $\Delta E$ , the more efficient the ion pairing.

In principle,  $E(\text{M}^+ \cdots \text{OH}_2)$  could be obtained from the mean value taking into account the whole solvation shell around the cation:  $-E(\text{M}^+ \cdots \text{OH}_2) \approx \Delta H_{\text{sol}}/n$ , where  $\Delta H_{\text{sol}}$  is the enthalpy of solvation and  $n$  the coordination number of the solvated cation. However, values of  $n$  reported in the literature depend strongly on the method of measurement.<sup>33</sup> Therefore we have estimated the energy of the bond between the cation and its hydrating waters from partial charge calculations using a cation bound to a single water molecule. Assuming an electron transfer involving the cation  $\text{M}^+$  and the lone electron pair of the oxygen atom of the water, the partial charge distribution and the bond length in the complex  $\text{M}^+ \cdots \text{OH}_2$  were calculated. The coulombic term of the bond energy was then deduced from  $E_{\text{C}} = Q(\text{M})Q(\text{O})/4\pi\epsilon_0 r$ , where  $Q(\text{M})$  and  $Q(\text{O})$  are the

(33) Amis, E. S.; Hinton, J. F. *Solvent Effects on Chemical Phenomena*; Academic Press: New York, 1973.

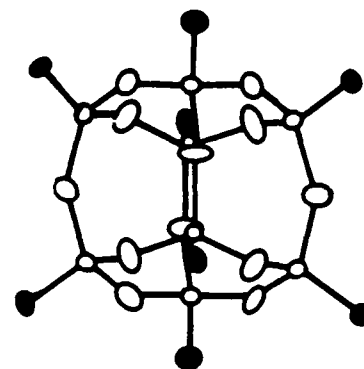


Figure 5. Structure of the silicate anion  $\text{Si}_3\text{O}_{20}^{8-}$  used in our charge distribution calculations. The oxygen atoms involved in the complexation with alkali-metal cations are filled in black.

Table II. Partial Charge Distribution for the Ion-Pair Complexes from the Cation  $\text{M}$  ( $\text{M} = \text{Li}, \text{Na}, \text{K}, \text{Rb}, \text{Cs}$ ) and the Silicate Fragment of Figure 5<sup>a</sup>

M	Q(M)	Q(O) <sup>b</sup>	Q(O) <sup>c</sup>	Q(Si)
Li	747	-550	-408	415
Na	768	-558	-411	407
K	842	-587	-422	379
Rb	859	-594	-425	373
Cs	888	-605	-429	362

<sup>a</sup> All the charges are given in  $10^{-3}e$  ( $e = 1.602 \times 10^{-19} \text{C}$ ). <sup>b</sup> Oxygen complexed with the metal  $\text{M}$ . <sup>c</sup> Oxygen in the bond  $\text{Si}-\text{O}-\text{Si}$ .

partial charges of the cation and oxygen, respectively,  $\epsilon_0$  is the vacuum permittivity, and  $r$  is the bond length. Since the electronegativity difference between the cation and the oxygen atom is so large, the Coulombic contribution is the only one considered.

The bond energy of  $\text{M}^+ \cdots \text{OSi}^-$  was estimated by a similar method. Using the charged silicate fragment shown in Figure 5, the cation is complexed to the negative oxygen atoms. This structure occurs in basic aqueous solutions of silicate salts and consists entirely of  $\text{Q}_3$  units, which are probably similar to  $\text{SiO}^-$  fragments on  $\text{SiO}_2$  colloidal gels.<sup>34</sup> The hybridization of the oxygen atoms has been adjusted for a  $\text{Si}-\text{O}-\text{Si}$  angle of about  $140^\circ$ . The calculated partial charges are shown in Table II.

The Coulombic energies of the bonds  $\text{M}^+ \cdots \text{OSi}^-$  and  $\text{M}^+ \cdots \text{OH}_2$  are given in Table III. The trend of these energies remains unaffected either by changing the number of complexed oxygen atoms in the silicate fragment or by using different silicate structures than the anion considered. Since we do not consider shielding and bonding by the rest of the solvation shell, the value of the hydration energy is not realistic. However, the trend of the hydration energy with cation size remains meaningful. The calculated partial charges for the  $\text{M}^+ \cdots \text{OSi}^-$  bonds are in reasonable agreement with values obtained from semi-empirical molecular orbital methods.<sup>36</sup>

The term  $\Delta E = -E(\text{M}^+ \cdots \text{OSi}^-) + E(\text{M}^+ \cdots \text{OH}_2)$  of the Gibbs enthalpy of the ion-pair reaction 10 was obtained by using the values for  $E(\text{M}^+ \cdots \text{OH}_2)$  and  $E(\text{M}^+ \cdots \text{OSi}^-)$  in Table III and is shown in Figure 6. The values of  $\Delta E$  calculated from formal charges and from the Allred-Ro-

(34) Iler, R. K. *The Chemistry of Silica*; Wiley: New York, 1979.  
(35) Kleinberg, J.; Argersinger, W. J.; Griswold, E. *Inorganic Chemistry*; Heath: New York, 1960.

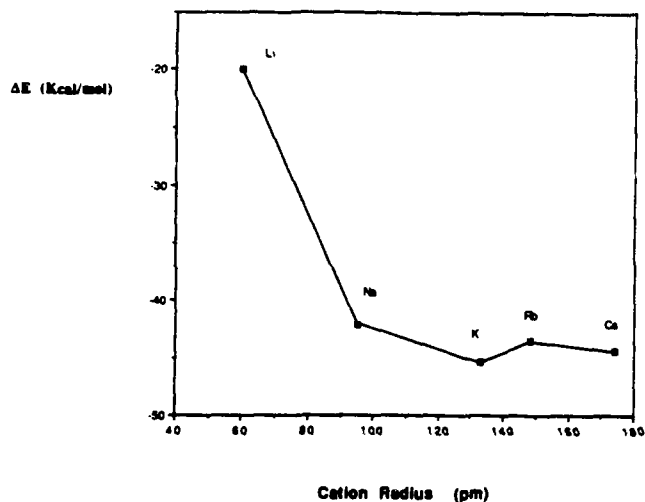
(36) De Jong, B. H. W. S.; Brown, G. E. *Geochim. Cosmochim. Acta* 1980, 44, 1627.

(37) McCormick, A. V.; Bell, A. T.; Radke, C. J. *J. Phys. Chem.* 1969, 93, 1733.

(38) Detallier, C. In *NMR of Newly Accessible Nuclei*; Lazzlo, P., Ed.; Academic Press: New York, 1983; p 105.

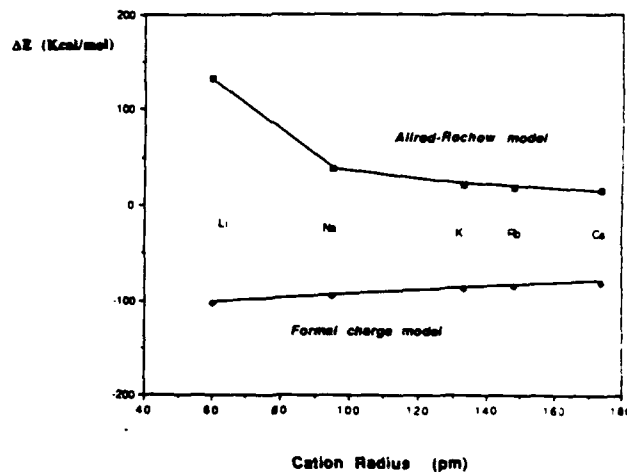
Table III. Estimated Coulombic Bond Energies and Bond Lengths for  $M^+ \cdots OH_2$  and  $M^+ \cdots OSi$ 

metal	ionic radius, <sup>a</sup> pm	$E(M^+ \cdots OH_2)$ , kcal/mol	$r(M^+ \cdots OH_2)$ , pm	$E(M^+ \cdots OSi)$ , kcal/mol	$r(M^+ \cdots OSi)$ , pm	$\Delta E$ , kcal/mol
Li	60	53.7	58.8	73.7	184.9	-20.0
Na	95	27.4	121.0	69.5	204.7	-42.1
K	133	21.4	174.4	66.8	245.9	-45.4
Rb	148	20.2	193.7	63.7	265.8	-43.5
Cs	174	18.3	222.2	62.7	284.6	-44.4

<sup>a</sup> From Kleinberg et al.<sup>35</sup>Figure 6. Curve of  $\Delta E$  vs ionic radius with  $\Delta E$  calculated from the bond orbital electronegativity equalization model.

chow model are presented in Figure 7. As can be seen in Figure 6, the experimental trend with a maximum in stability for potassium complexation is reasonably well predicted with the bond orbital electronegativity equalization model. On the contrary, if the Coulombic bond energies are calculated considering formal charges on the oxygen atom and the metal, no maximum of stability is predicted for potassium ion-pair complexes. Likewise, the Allred-Rochow model does not fit the experimental trend (Figure 7).

It appears that the ion-pair equilibrium results from the balance between solvation of the cation and strength of the ion-pair bond. For instance, though the  $Li^+ \cdots OSi$  bond is the strongest,  $Li^+$  is so strongly solvated that the ion pairing is less favorable compared with the other cations. Furthermore, the  $K^+ \cdots OSi$  bond is more favored than might have been expected since  $K^+$  holds the hydrating water less tightly and at the same time the  $K^+ \cdots OSi$  bond is strong enough. Potassium represents thus the best compromise with its moderate size and its low electronegativity. The experimental trend, and in particular the high stability of the potassium ion pair, is thus explained

Figure 7. Curve of  $\Delta E$  vs ionic radius with  $\Delta E$  calculated from the Allred-Rochow model and a formal charge model.

by our calculations, at least qualitatively.

### Conclusion

It has been shown that ion-pairing complexation between cations and charged silicate groups occurs in basic conditions in the condensation of TEOS-derived oligomeric structures, supporting the condensation mechanism proposed by McCormick et al.<sup>4</sup> NMR spectroscopy reveals that the cation, initially solvated by water, can bind directly to a colloidal silica particle.

The relative efficiency of ion pairing and the trend in ion-pair exchange agree well with a model based on the Bergmann-Hinze method of charge distribution calculations.<sup>1</sup> This reaction model assumes that charged silicate groups compete with waters of hydration to coordinate the cation.

**Acknowledgment.** J.S. was supported by NSF Grant CBT-8910423. This material is based upon work supported by this grant.

**Registry No.** Li, 7439-93-2; Na, 7440-23-5; K, 7440-09-7; Rb, 7440-17-7; Cs, 7440-46-2; tetraethoxysilane, 78-10-4; silicate, 12627-13-3.

DTIC QUANTITY UNLIMITED 3

Accession Codes	
Dist	Avail and/or Special
A-1	20